



PAPER • OPEN ACCESS

# Characterisation of hydrophone sensitivity with temperature using a broadband laser-generated ultrasound source




To cite this article: Marina Bakaric *et al* 2023 *Metrologia* **60** 055002

View the [article online](#) for updates and enhancements.

## You may also like

- [Using a heterodyne vibrometer in combination with pulse excitation for primary calibration of ultrasonic hydrophones in amplitude and phase](#)  
Martin Weber and Volker Wilkens
- [Multivariate control charts for calibration of hydrophones using the Mahalanobis statistic](#)  
S E Crocker, W H Slater and M A Bergeron
- [Frequency characteristics of receiving sensitivity and waveform of an anti-acoustic cavitation hydrophone](#)  
Michihisa Shiiba, Nagaya Okada, Takeyoshi Uchida et al.

# Characterisation of hydrophone sensitivity with temperature using a broadband laser-generated ultrasound source

Marina Bakaric<sup>1,2,4</sup> , Olumide Ogunlade<sup>1,3</sup>, Piero Miloro<sup>1,2</sup> , Bajram Zeqiri<sup>1,2</sup>, Benjamin T Cox<sup>1</sup> and Bradley E Treeby<sup>1,\*</sup> 

<sup>1</sup> Department of Medical Physics and Biomedical Engineering, University College London, London, United Kingdom

<sup>2</sup> Medical, Marine and Nuclear Department, National Physical Laboratory, Teddington, United Kingdom

<sup>3</sup> Wellcome/EPSRC Centre for Interventional and Surgical Sciences, University College London, London, United Kingdom

E-mail: [b.treeby@ucl.ac.uk](mailto:b.treeby@ucl.ac.uk)

Received 15 February 2023, revised 23 June 2023

Accepted for publication 4 July 2023

Published 28 July 2023



CrossMark

## Abstract

In this work, we present a novel method for characterising the relative variation in hydrophone sensitivity with temperature, addressing a key aspect of measurements in the field of ultrasound metrology. Our study focused on a selection of miniature ultrasonic hydrophones commonly used in medical applications. The method is based on using water as a temperature-sensitive laser-generated ultrasound (LGUS) source for calibration, allowing for flexible characterisation across a wide temperature range. The measurements were performed using both the LGUS method and the established self-reciprocity method. Our results demonstrate good agreement within 5% between the two methods, validating the effectiveness of the LGUS approach. We found that the sensitivity of the tested hydrophones exhibited low temperature dependence less than  $-0.2\%$  per  $^{\circ}\text{C}$  within the studied temperature range from  $17^{\circ}\text{C}$  up to  $50^{\circ}\text{C}$ . The presented LGUS method offers greater flexibility than current approaches as it allows for characterisation of membrane hydrophones with small element sizes and non-electrical transducers. By combining the relative sensitivity variation obtained through the LGUS method with the standard calibration at room temperature, absolute values of hydrophone sensitivity can be determined. The expanded uncertainty of our measurements, which was evaluated at temperature intervals of  $8^{\circ}\text{C}$ , was determined to be on average 10%. Our work provides valuable insights into the temperature dependence of hydrophone sensitivity and lays the foundation for further investigations in this area. The LGUS method holds promise for future enhancements, such as increased bandwidth of the LGUS source and frequency domain analysis, to explore the frequency dependency of sensitivity variation with temperature.

<sup>4</sup> Present address: Precision Acoustics Ltd Hampton Farm Business Park, Higher Bockhampton, Dorchester, DT2 8QH, United Kingdom.

\* Author to whom any correspondence should be addressed.



Original Content from this work may be used under the terms of the [Creative Commons Attribution 4.0 licence](https://creativecommons.org/licenses/by/4.0/). Any further distribution of this work must maintain attribution to the author(s) and the title of the work, journal citation and DOI.

Keywords: calibration, hydrophone, laser generated ultrasound, metrology, photoacoustics, sensitivity, temperature.

(Some figures may appear in colour only in the online journal)

## 1. Introduction

### 1.1. Overview

Miniature ultrasonic hydrophones are a type of measurement device commonly used to characterise the properties of an acoustic field. The procedures in which the acoustic sensitivity of each device is calibrated, and subsequent methods in which these devices can be utilised to specifically measure acoustic fields generated by medical equipment in liquids are detailed in the following standards: IEC 62127-1:2022 [1] and IEC 62127-2:2007 [2]. In an ideal case, the temperature of the environment in which the hydrophone is intended for should be suitably similar to the temperature under which the hydrophone was calibrated. Acoustic output measurements, however, are routinely conducted at a room temperature of  $22\text{ }^{\circ}\text{C} \pm 3\text{ }^{\circ}\text{C}$  [3]. From their design, hydrophones are known to have intrinsic electroacoustic properties which have variance with temperature [4]. If hydrophone sensitivity and frequency response data at an alternative temperature is of interest, a set of limited corrections and adjustments can be applied. It has been identified that literature surrounding this conversion is scarce, covering only a temperature range between  $16\text{ }^{\circ}\text{C}$  and  $24\text{ }^{\circ}\text{C}$  [5].

The knowledge of the variation in hydrophone sensitivity with temperature is important in applications such as acoustic material characterisation and use of hydrophones for mapping transducers at body temperature, when the temperature of the water bath is different from the one used for calibration. It would also benefit international comparisons of hydrophone calibrations [6, 7].

Recently, the effect of temperature from  $50\text{ }^{\circ}\text{C}$  to  $130\text{ }^{\circ}\text{C}$  on the performance of poly-vinylidene fluoride (PVDF) film transducers was investigated [8, 9]. The transducers were fabricated from uniaxially stretched and poled PVDF films of various thicknesses, laminated between two steel discs functioning as electrodes and connected to  $50\text{ }\Omega$  coaxial cables with a PTFE coated wire. During the measurements, the transducers were placed in a temperature-regulated oil bath. Pulse-echo responses were acquired from a reflector positioned 10 mm away at various temperatures between 18 and  $130\text{ }^{\circ}\text{C}$  over a duration of 5 hours. The results showed all transducers exhibited an initial drop in sensitivity when exposed to temperatures of  $60\text{ }^{\circ}\text{C}$  and above, followed by an extended slow decline. Although these findings provide valuable qualitative insight into the effect of temperature on PVDF transducers such as miniature ultrasonic hydrophones, their variation in sensitivity will be affected by not only the PVDF film thickness, but also the design, electrical impedance matching and other factors. Thus a technique by which the sensitivity of any transducer can be directly measured as a function of temperature is necessary.

### 1.2. Hydrophone calibration methods

The temperature dependence of hydrophone sensitivity has previously been measured for temperatures between  $16\text{ }^{\circ}\text{C}$  and  $24\text{ }^{\circ}\text{C}$  using the NPL Primary Standard Laser Interferometer [4, 5]. In this study, a coplanar-shielded membrane hydrophone showed a relative variation in sensitivity of  $6.5 \times 10^{-3}\text{ }^{\circ}\text{C}^{-1}$  (approximately 6% over the temperature range), while a bilaminar-shielded membrane hydrophone showed a smaller variation (less than  $2.5 \times 10^{-3}\text{ }^{\circ}\text{C}^{-1}$  or approximately 2% over the measurement range). The primary calibration of hydrophones is typically based on optical interferometric techniques which determine the displacement of a thin pellicle within the far-field of an ultrasound transducer or at the focus of a focusing transducer, which is proportional to the applied pressure [10, 11]. The pellicle is then substituted with a membrane hydrophone and the electrical signal from the device is acquired in the same position of the field [12, 13]. As the acoustic field is the same for the pellicle and the hydrophone, this method can be used to determine the variation in sensitivity of a hydrophone with changes in water temperature, without introducing errors caused by the sensitivity of the ultrasonic source transducer to temperature variations [4]. However, these measurements can only be performed in a handful of specialised laboratories in the world. They also require each of the measurement components (e.g. transmission of the pellicle, interferometer laser spot size, etc) to be known at each temperature the hydrophone is calibrated (IEC 62127-2:2007 Annex F [2]). For this reason, most primary hydrophone calibrations are performed in a temperature controlled environment close to  $20\text{ }^{\circ}\text{C}$ . Other secondary hydrophone calibration techniques based on the substitution or comparison principle [14] will comprise the difficulty of the temperature dependence of the source transducer sensitivity, and may provide only relative differences between the substituted hydrophones when applied to investigations of temperature dependency.

The self-reciprocity calibration method uses the theory of acoustic transduction and propagation in an electroacoustic transducer to generate a known acoustic pressure field without the need for a primary standard or standard transducer [15]. The hydrophone being calibrated is used as both a transmitter and receiver. It emits an ultrasonic tone burst onto a reflector and subsequently receives the reflected signal. The quantities measured are electrical and absolute values of pressure can be determined with low uncertainties by using specialised equipment and applying knowledge of all the components' uncertainties. The technique also requires minimal geometrical adjustment to be carried out and is suitable for a relative measurement of temperature-dependent variation in hydrophone sensitivity by changing the water bath temperature.

However, calibration by self-reciprocity is not applicable to all hydrophones. Generally, hydrophones of the type used for the characterisation of medical ultrasonic fields which are made from piezopolymers (such as PVDF) do not produce sufficient acoustic output due to their small element size and thus cannot be calibrated using this technique. The minimum diameter for a practical transducer is about 2 mm [2], while the hydrophones most commonly used when characterising medical ultrasound devices have a diameter smaller than 0.5 mm. Additionally, modern hydrophone systems comprise an integrated preamplifier whose electronics impede the application of the hydrophone as an acoustic source. This calibration method also cannot be applied to non-electrical transducers such as those used in optical sensing [16].

### 1.3. Paper outline

In this paper, a novel method for characterising the relative variation in hydrophone sensitivity with temperature is presented. The method is based on using water as a laser-generated ultrasound (LGUS) source, and was used to investigate the variation in hydrophone sensitivity from 17 °C up to 50 °C for three different hydrophones, including the 1.0 mm bilaminar membrane hydrophone from the original 1999 study [4]. A custom-made broadband PVDF receiver with a 5 mm active element was used in a validation study, where its change in sensitivity with temperature was characterised using the self-reciprocity method [15].

The principle of LGUS and the method for characterising the temperature-dependent sensitivity of a hydrophone are described in section 2. The validation study using self-reciprocity is outlined in section 3, followed by the study findings (section 4). The results are discussed and summarised in section 5.

## 2. Methods

### 2.1. Principle of LGUS

A pulse of light incident on an absorbing sample is scattered and absorbed, consequently resulting in a rise in pressure (and subsequent relaxation in the form of thermal expansion) [17]. In cases where the scattering is much weaker than absorption, the light distribution in a sample along the axial direction of the excitation beam at normal incidence can be described by Lambert's law as:

$$\Phi(z) = \Phi_0 e^{-\mu_a z} U(z) \tag{2.1}$$

where  $U$  is the Heaviside step function defined as:

$$U(z) = \begin{cases} 1, & z \geq 0 \\ 0, & z < 0 \end{cases} \tag{2.2}$$

and  $\Phi(z)$  is the depth-dependent fluence distribution,  $\Phi_0$  is the fluence incident on the sample surface, and  $\mu_a$  is the optical absorption coefficient [17].

If the optical pulse duration is much shorter than the thermal and stress relaxation times of the material, and assuming all absorbed optical energy decays into heat, a thermoelastic stress wave is induced which then propagates away from the heated volume [18]:

$$p_0(z) = \mu_a \Gamma \Phi_0 e^{-\mu_a z} \tag{2.3}$$

where  $p_0(z)$  is the depth dependent pressure distribution at time  $t = 0$ ,  $z$  is the depth and  $\Gamma$  is the Grüneisen parameter or thermoelastic efficiency.  $\Gamma$  is a dimensionless parameter describing the conversion efficiency between the absorbed optical energy and acoustic pressure [19], and for a homogeneous fluid can be related to other thermodynamic properties as:

$$\Gamma = \frac{\beta c^2}{C_p} \tag{2.4}$$

where  $\beta$  is the coefficient of volume thermal expansion,  $C_p$  is the specific heat under constant pressure and  $c$  is the speed of sound in water. The properties of the induced acoustic pulse depend on the optical pulse duration and energy, the size of the illuminated region, and the physical properties of the medium. One such property is the product  $\mu_a \Gamma$  called the photoacoustic conversion efficiency, an intrinsic material property which determines the amplitude of the wave. This principle can be used to generate ultrasound waves, and control their amplitude, bandwidth and spatial size [20]. Ultrasound waves generated in this manner are often referred to as LGUS [21].

When a hydrophone is placed in the water at a distance  $z = d$  from the source, the pressure of an LGUS wave as recorded by the hydrophone  $V(t)$  can be described as:

$$V(t) = S \mu_a \Gamma \Phi_0 e^{-\mu_a(d-ct)} e^{-\alpha ct} H(z-ct) \tag{2.5}$$

where  $S$  is the hydrophone sensitivity, and  $\alpha$  is the acoustic attenuation coefficient of water expressed in  $\text{Np m}^{-1}$  [18]. Provided the LGUS properties are known as a function of temperature, the change in the hydrophone's sensitivity with temperature  $T$  can be calculated from the change in the peak of the recorded time series occurring at  $t = d/c$ , corrected for the temperature-dependent source properties. A relative measure of this variation can be obtained by normalising the sensitivity at temperature  $T$  to that at room temperature  $T_0$ :

$$\frac{S(T)}{S(T_0)} = \frac{\mu_a(T_0) \Gamma(T_0)}{\mu_a(T) \Gamma(T)} \frac{e^{\alpha(T)d}}{e^{\alpha(T_0)d}} \frac{V_{\max}(T)}{V_{\max}(T_0)}. \tag{2.6}$$

Here,  $\mu_a(T)$  is retrieved by performing curve-fitting to the decaying exponential part of the recorded photoacoustic signal,  $\Gamma(T)$  and  $\alpha(T)$  can be obtained from the literature, while  $V_{\max}$  is the measured peak positive voltage of the detected signal. The expression is derived from equation (2.5) where  $\Phi_0$  cancels out as it is independent of temperature for a non-scattering fluid such as water. If this is obtained over a significantly wide temperature range, a temperature correction factor for hydrophone sensitivity can be acquired and subsequently

used to correct the absolute hydrophone sensitivity at temperature  $T_C$  from the sensitivity obtained at a different temperature  $T$  from a standard hydrophone calibration. Provided the relationship between the hydrophone sensitivity and temperature is linear within the measurement temperature range, a temperature correction factor  $a$  can be defined as the slope of the measured trend in hydrophone sensitivity with temperature, expressed in percentage per degree celsius:

$$a = \frac{\Delta S}{\Delta T} \times 100 \quad (2.7)$$

and sensitivity corrected as:

$$S(T) = S(T_C) + a(T - T_C). \quad (2.8)$$

## 2.2. LGUS source

The last decade has seen a rise in the development and use of LGUS sources. These sources are usually comprised of nanocomposite materials, which when excited by a short pulse of laser light produce a broadband, high amplitude ultrasound pulse. Such a source was recently developed as a calibration source for hydrophone calibrations up to 100 MHz [21]. However, in order to investigate the effect of temperature on hydrophone sensitivity using the theory outlined above, the temperature dependence of the LGUS source properties must be well-characterised or known *a priori*. The simplest example of such a material is water.

Water has been used as a standard medium in various measurements, and its properties are well known. The temperature dependence of the speed of sound in water within the limits from 0 °C to 95 °C can be described by a fifth-order polynomial given by Marczak [22], while its acoustic absorption coefficient is described by a seventh-order polynomial fitted to the data given by Pinkerton [23]. For temperatures between 4 °C and approximately 70 °C (over which the speed of sound in water increases with temperature) the Grüneisen parameter of water can be approximated as  $\Gamma(T) = 0.0053T + 0.0043$  [24], where this linear relation was derived from its definition (equation (2.4)) and knowledge of the temperature dependence of the speed of sound, volume thermal expansion coefficient and specific heat capacity at constant pressure for water and aqueous solutions.

In order to efficiently use water as a LGUS source, the laser light must be tuned to one of the water's absorption peaks. The water's optical absorption spectrum in the visible to infrared spectral region is dominated by the fundamental rotational and vibrational modes of the water molecule [25]. Specifically, the dominant vibrational features of the two O-H bonds lead to major absorption maxima, where each of these modes is predominant at a certain wavelength thus giving rise to the absorption peaks in the spectrum [26]. Absorption peaks in the infrared (IR) and near-infrared (NIR) optical spectrum of water occur around 1460 nm, 1940 nm and 2950 nm [27, 28]. The exact wavelength and  $\mu_a$  value vary depending on water processing and quality, as well as measurement method and

wavelength resolution [29]. Considering the wavelength range of the lasers available in the Photoacoustic Imaging Group at UCL, the 1460 nm peak was chosen as the target wavelength. While Irvine and Pollack report  $\mu_a = 26 \text{ cm}^{-1}$  at 1450 nm [30], Hale and Quarry have measured values of  $28.8 \text{ cm}^{-1}$  and  $28.4 \text{ cm}^{-1}$  at 1440 nm and 1460 nm, respectively [27]. Palmer and Williams have reported a value of  $28.5 \text{ cm}^{-1}$  at 1471 nm [28]. No information, however, was given on the measurement temperature.

## 2.3. Measurement setup

Using the theory outlined above, a setup for measuring the variation in hydrophone sensitivity with temperature as defined in equation (2.6) was designed using water as a laser-generated ultrasound source. The main parts of the measurement setup, shown in figure 1, comprised of a light source (1), a water bath (2) with temperature control (3), custom-made hydrophone mount and the hydrophone being calibrated (4).

A tunable fiber-coupled Nd:YAG pumped OPO laser (Spitlight 600, InnoLas Laser GmbH, Krailling, Germany) was used for the generation of LGUS signals in water, with a pulse duration 4 ns and pulse repetition frequency of 30 Hz. The laser source was coupled to an optical fibre with a numerical aperture of approximately  $20^\circ$  (1). The beam was geometrically spread to a diameter of approximately 20 mm at the tank's optical window (2.b). In order to determine the absorption peak of degassed deionised water as used in the measurement setup, a wavelength sweep from 1400 nm to 1600 nm in steps of 10 nm was done. The water was treated with an in-house system (Purelab Option-R 7/15, ELGA LabWater, High Wycombe, U.K.) and its conductivity measured at the beginning of the experiment using a conductivity meter (CON450, Eutech Instruments, Singapore) and was  $0.80 \mu\text{S}$ . The water temperature was 19 °C. Figure 2 shows the relative water absorption spectrum as measured in-house, with the water absorption peak occurring at 1470 nm. The optical absorption coefficient of water at 1470 nm changes by 6% from 18 °C to 50 °C, and this change was taken into account when calculating the change in hydrophone sensitivity with temperature [31].

The water bath consisted of a tank (2.a) with an optical window (2.b) and an acoustic absorber (2.c) placed behind the hydrophone. The tank was manufactured from Poly(methyl methacrylate) (PMMA), with inner dimensions of  $245 \text{ mm} \times 245 \text{ mm} \times 390 \text{ mm}$  (height  $\times$  width  $\times$  length). The optical window was a 30 mm diameter circular IR quartz window (IRQ-302, UQG Ltd Cambridge, U.K.). A 10 mm thick PMMA slab was used as a partition for adjusting the tank length and volume of water being heated.

The temperature control was achieved using a thermostat with an external circulation (ECO RE415S Silver thermostat, Lauda Dr R. Wobser GmbH, Lauda-Königshofen, Germany) connected to two aluminium heating elements immersed in

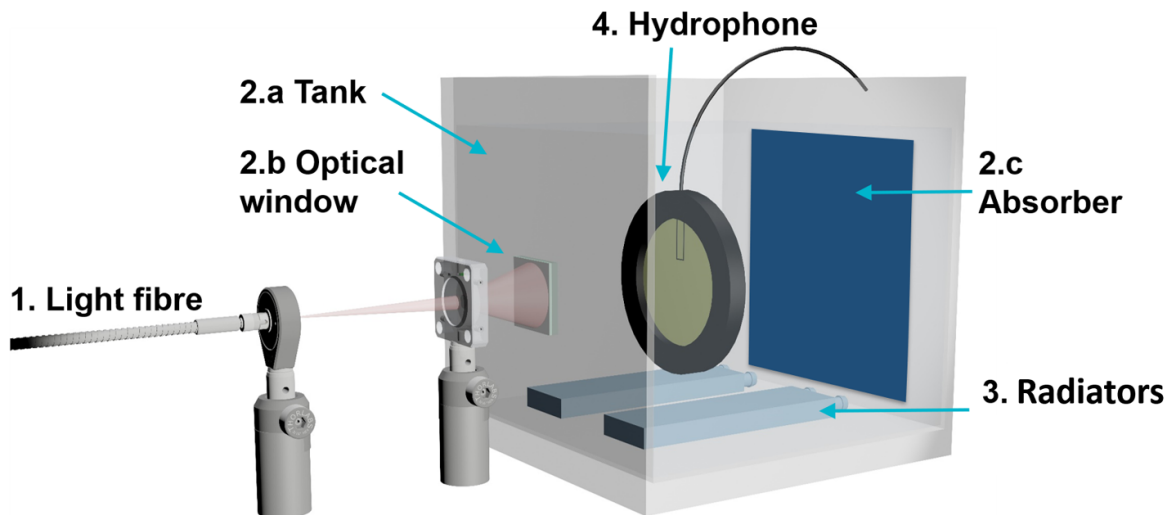


**Figure 1.** Setup for hydrophone calibration using a LGUS source. Light is delivered through the optical fibre (1) into the tank (2.a) through an optical window (2.b). The water temperature is regulated via two heating elements (3) connected to a thermostat and the generated photoacoustic signals recorded by a hydrophone (4).

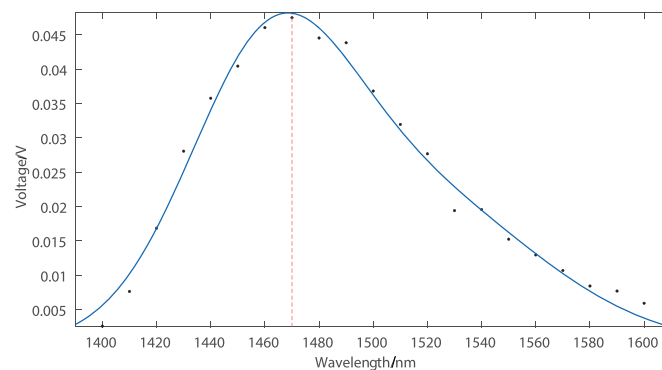


**Figure 2.** Relative absorption spectrum of deionised water between 1400 nm and 1600 nm, where the points represent the measured data, while the blue line is a fitted curve. The absorption peak occurs at 1470 nm.

the tank (3). Temperature feedback was received using a T-type thermocouple (5TC-TT-TI-36-1 M-SMP-M IEC PFA-insulated, Omega Engineering Limited, Manchester, U.K.) positioned close to the hydrophone.

The hydrophone being calibrated (4) was sandwiched between two PMMA rings with an acoustic window of 90 mm and mounted on a custom-built rig with two translation stages on each side of the tank to enable precise hydrophone positioning with an accuracy of 0.01 mm in two degrees of freedom. The hydrophone was connected to an oscilloscope (DSO-X 3024A, Agilent Technologies, Palo Alto, CA, USA) and signal acquisition triggered using an in-house built photodiode and waveforms digitised with a sampling frequency of 200 MHz and 2000 averages.

#### 2.4. Hydrophones

In this study, two membrane hydrophones were characterised: a 1.0 mm bilaminar membrane hydrophone (S/N IP033,

GEC-Marconi Electronics Ltd UK) from the 1999 study by Preston *et al* [4] and a 0.2 mm differential membrane hydrophone (S/N D0902, Precision Acoustics Ltd Dorchester, UK). The sensitivity of these hydrophones has been measured in the National Physical Laboratory secondary standard measurement system [32] in the range (1–40) MHz and a room temperature of  $20\text{ }^{\circ}\text{C} \pm 0.5$ . The sensitivity at 1 MHz is  $91\text{ nV Pa}^{-1}$  and  $99\text{ nV Pa}^{-1}$  for the Marconi and the Precision Acoustics hydrophone, respectively. The Marconi bilaminar hydrophone was connected to the oscilloscope using a  $1\text{ M}\Omega$  IN– $50\text{ }\Omega$  OUT amplifier. The differential hydrophone features a differential input preamplifier embedded into the hydrophone ring and was connected to a power supply. The signals recorded from both hydrophones were amplified using a hydrophone booster amplifier (MA2, Precision Acoustics Ltd Higher Bockhampton, U.K.).

The hydrophone used in the validation study was a custom-made circular plane piston, immersion hydrophone providing a flat, broadband sensitivity (S/N PA1075, Precision Acoustics



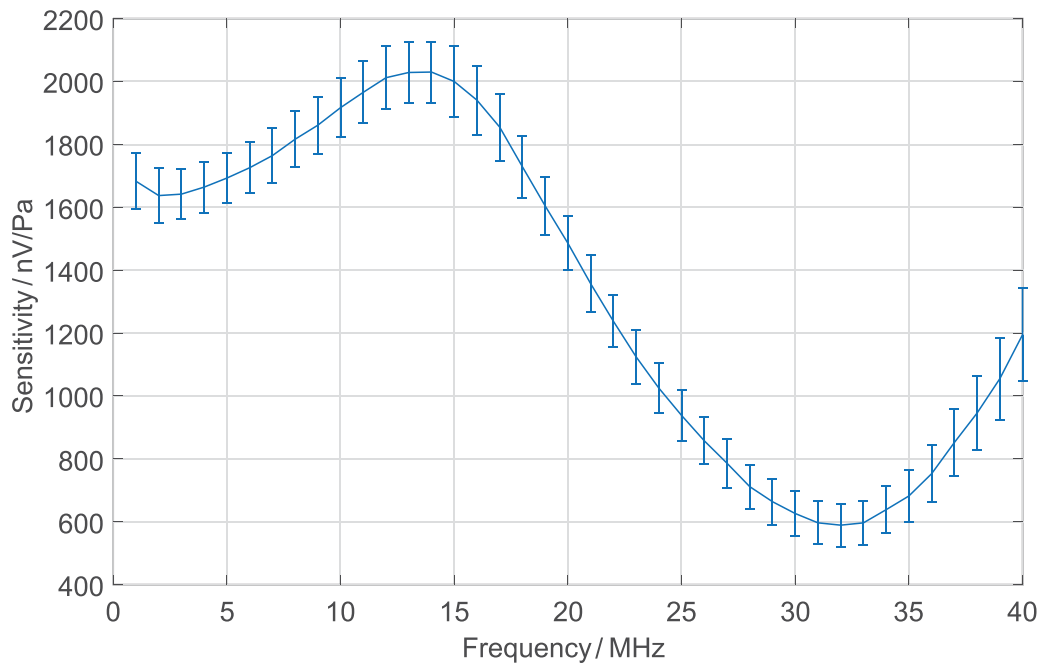


**Figure 3.** Frequency response of the PA1075 hydrophone in the range 1 MHz to 40 MHz. The uncertainty bars represent the expanded uncertainty ( $p = 0.95$ ).

Ltd Dorchester, UK). The hydrophone is made from a 28  $\mu\text{m}$  PVDF film, has an acoustically hard backing made of tungsten/epoxy composite and an acoustic aperture of 23 mm. The hydrophone has a 5 mm active element and a centre frequency of 14 MHz. The hydrophone was connected to the oscilloscope using a hydrophone preamplifier with a 9 dB voltage gain, which also buffers the signal and provides a 50  $\Omega$  output. The amplifier is powered by a DC coupler. The free-field sensitivity of the hydrophone at room temperature of 22  $^{\circ}\text{C}$  was measured across the frequency range from 1 MHz to 40 MHz at the NPL Hydrophone Calibration facility [32]. A comparison method was used where the response of the test hydrophone was compared against a reference transfer standard hydrophone, the calibration of which is traceable back to the NPL Primary Standard laser interferometer [4]. Spatial averaging corrections were applied to compensate for the different diameter between the reference and test device [33]. The hydrophone's sensitivity as a function of frequency is shown in figure 3. It has a peak sensitivity of 2030  $\text{nV Pa}^{-1}$  at its centre frequency of 14 MHz. The expanded uncertainty at this frequency is 5.2%.

### 2.5. LGUS setup simulation

In order to determine the distance between the LGUS source and the hydrophone required to resolve the direct ultrasound wave from any edge waves, an axisymmetric time-domain simulation of wave propagation (using `kspaceFirstOrderAS` function [34] in `k-Wave` [35]) was performed. The simulation was run for each hydrophone separately as the required source-hydrophone separation depends on the hydrophone's active element size. A snapshot of the simulation is shown in figure 4(a). A cylindrical LGUS source

with the radius of 10 mm was defined as a 1D decaying exponential with a constant optical absorption coefficient of  $28.5\text{e}+02 \text{ m}^{-1}$  corresponding to the water absorption peak value at 1470 nm reported in the literature [27, 28]. The sensor radius was defined as half the hydrophone's active element size and pressure recorded with a line across the sensor. During the simulations, the medium speed of sound (and thus effectively its temperature) was varied within the intended temperature range for the hydrophone calibration, while the source-sensor separation distance was varied between 15 mm and 55 mm in steps of 10 mm. An example of the simulated waveforms at temperatures of 17  $^{\circ}\text{C}$  and 50  $^{\circ}\text{C}$  for the PA1075 hydrophone with an active element radius of 2.5 mm is shown in figure 4(b). The recorded pressure values can be considered arbitrary as the simulation is linear and the findings thereof were used solely to investigate the effect of source-hydrophone distance on the recorded signal shape.

It can be seen that for separation distances greater than 25 mm the edge wave is overlapping with the main wave and affecting the signal amplitude. Reducing the distance between the LGUS source and hydrophone separates the edge waves from the main wave and ensures an accurate signal amplitude is recorded. The maximum required separation distance suitable for all three hydrophones was 25 mm. An alternative method to derive an appropriate geometrical setting could be derived by spatial impulse response considerations as discussed in IEC 62127-2 [2], clause G.5.

### 2.6. Protocol for hydrophone calibration using an LGUS source

During the measurements, the entire setup was placed in a light-absorbing enclosure for eye-safety purposes. The tank

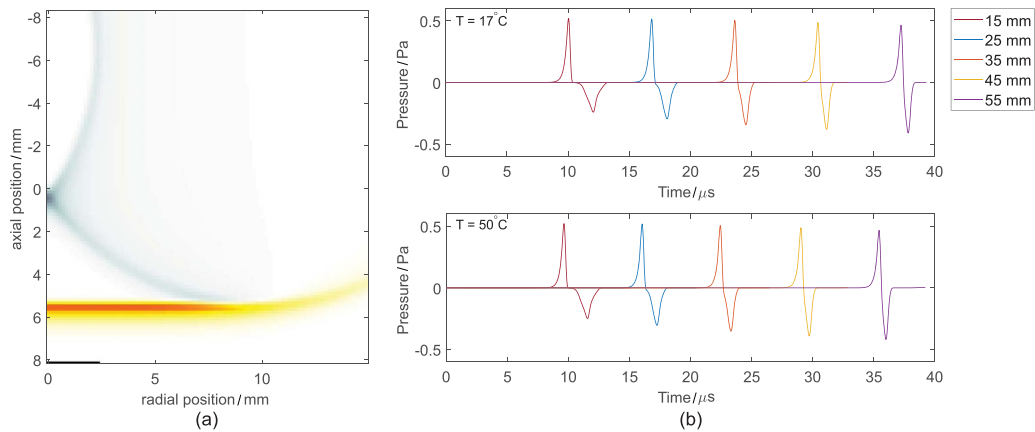


**Figure 4.** Axisymmetric simulation of the LGUS source. (a) Simulation snapshot with the black line representing the sensor mask, red-yellow line the incoming ultrasound wave, and blue lines the edge waves. (b) Simulated waveforms at  $17^\circ\text{C}$  and  $50^\circ\text{C}$  for source–sensor separation distances between 15 mm and 55 mm. The recorded pressure values are arbitrary.

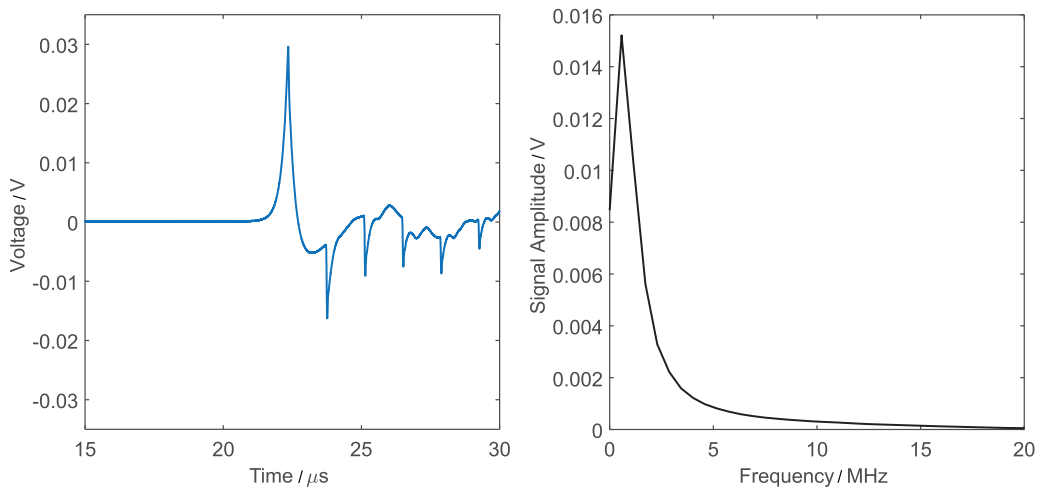


**Figure 5.** An example of a LGUS signal as recorded by the PA1075 hydrophone (left) at  $20^\circ\text{C}$  and the corresponding single-sided amplitude spectrum (right).

was filled with degassed deionised water as used in the water absorption peak measurement described in section 2.2. The water was deionised to reduce the build-up of mineral deposits on the tank and equipment, stop electrical conduction through the water and ensure consistent medium properties throughout the measurements. Degassing reduces the probability of bubble formation during the experiment [36] and was achieved by boiling the water.

The hydrophone being calibrated was placed in the holder, immersed in water and aligned for maximum signal. The water (and thus hydrophone) temperature was changed in the range between  $17^\circ\text{C}$  to  $50^\circ\text{C}$  (depending on the permitted range for the hydrophone being calibrated according to the manufacturer), and signals acquired every  $1^\circ\text{C}$  during both heating and cooling. The measurement was repeated five times, where a measurement constitutes of data acquisition during both heating and cooling cycles, thus making a total of 10 data sets for each of the three hydrophones.

## 2.7. Data processing

The data acquired using the LGUS method was processed assuming all frequency components have the same temperature dependencies. The recorded time-domain signals were processed in MATLAB (R2020a, MathWorks, Massachusetts, USA) by first averaging the data and removing any DC offset. An example of the signal recorded by the PA1075 hydrophone and the corresponding amplitude spectrum are presented in figure 5 for reference. The spectrum was acquired by applying a zero-padded fast Fourier transform to the signals and the single-sided amplitude  $A(f)$  spectrum obtained as a function of frequency  $f$  is shown here for illustration only.

The initial part of the signal corresponds to the initial pressure distribution, which is proportional to the axial distribution of the absorbed energy in the irradiated volume. The positive peak of the signal corresponds to the absorbed energy at the interface between the optical window and the water. The negative peak is caused by edge waves from the perimeter



of the excitation beam [17]. This is followed by reverberations caused by multiple acoustic or light reflections in the optical window, which were removed during post-processing by windowing the data. The photoacoustically generated peak pressure at 20 °C was in the order of 25 kPa and was measured using a calibrated piston hydrophone (PA1075) used in the validation study. For hydrophones with lower sensitivity, higher pressures might be required for the calibration. The signal amplitude spectra as shown in figure 5 indicates the majority of the signal is contained around 1 MHz. Equation (2.6) can thus be simplified as the ratio  $\frac{e^{\alpha(T)d}}{e^{\alpha(T_0)d}}$  for a maximum measurement temperature of 50 ° and a baseline of 17 °C in water is approximately equal to 1 (0.9997) for a frequency of 1 MHz and separation distance 25 mm. Thus the change in the measured peak only needs to be corrected for  $\mu_a(T)$  and  $\Gamma(T)$ , a detailed description of which can be found in [31].

2.8. Measurement uncertainty

Measurement uncertainty was evaluated following the guide to the expression of uncertainty in measurement [37]. The expanded measurement uncertainty as quoted in the results section was determined using both Type A (random) and Type B (systematic) uncertainty evaluations. This is given as the standard uncertainty multiplied by a coverage factor,  $k = 2$ , providing a coverage probability of approximately 95% ( $p = 0.95$ ), according to the methods recommended in [37, 38]. Contributions of Type A uncertainties were evaluated at intervals of 8 degrees Celsius (22 °C, 30 °C, 38 °C and 46 °C), while Type B uncertainties arise from several sources not affected by the temperature changes in the water bath. These were independently evaluated or quoted from the available literature, as briefly described in table 1. These included laser noise, oscilloscope linearity and resolution, and contributions of uncertainty in the optical absorption coefficient used to calculate the hydrophone sensitivity.

3. Validation

3.1. Principle of self-reciprocity

In order to validate the results obtained using the above-described LGUS method, the self-reciprocity method was used [15]. The method was adapted to include a relative measurement of the hydrophone’s sensitivity over a wide temperature range. As outlined in section 1.2, this method uses the theory of acoustic transduction and propagation to generate a known acoustic pressure field by using the hydrophone being calibrated as both a transmitter and receiver. Here, a reciprocal coefficient for plane waves  $J_p$  is defined as the ratio of the free-field sensitivity  $M$  and the transmitting current response  $S$  of the hydrophone:

$$\frac{M}{S} = \frac{UI}{p^2} = \frac{2A}{\rho c} = J_p. \tag{3.1}$$

**Table 1.** Uncertainty sources and their contributions ( $k = 1$ ), expressed as a percentage (%). Sources correlated with temperature are labelled with †.

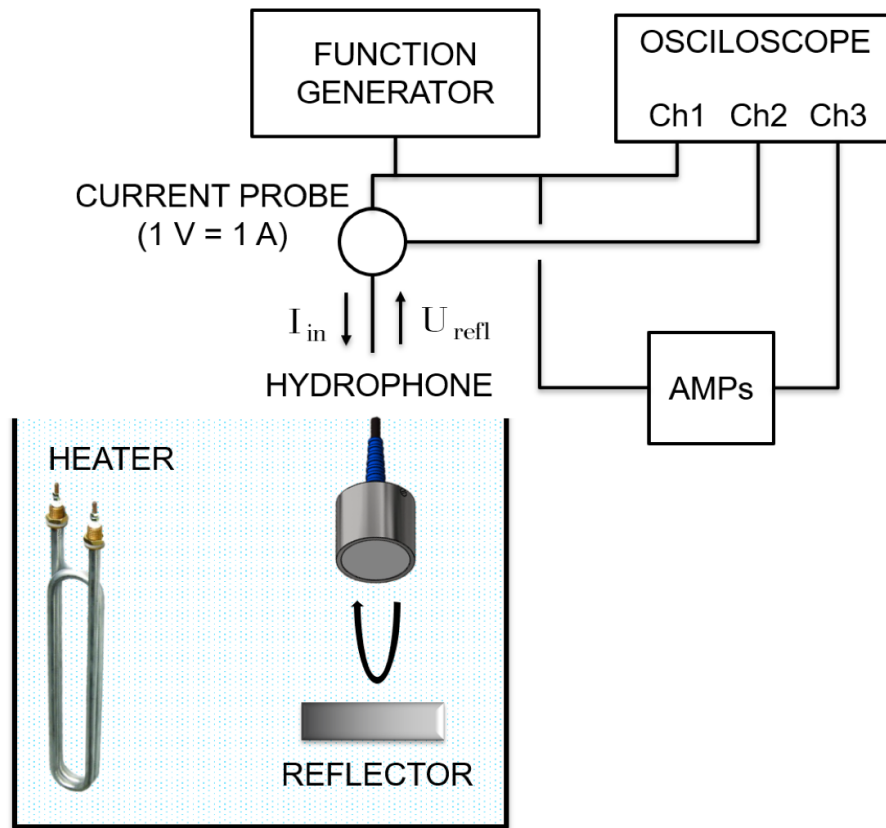
Source of uncertainty	Standard uncertainty (%)	Description
Type A	2.5 <sup>a</sup>	Random/repetitions.
Laser shot-to-shot noise	0.08	Evaluated from laser power output measurements over 300 averages.
Laser stability RMS	1.50	From laser specifications.
Laser photodiode	0.46	From [10]
Distance dependence of the field <sup>†</sup>	1.48	Evaluated from k-Wave simulations by taking the percentage difference in amplitude at 18 °C and 50 °C
Oscilloscope linearity and distortion	1.00	From oscilloscope specifications.
Oscilloscope resolution	0.40	From oscilloscope specifications.
Hydrophone preamplifier linearity	1.00	From specifications.
Signal-to-noise	0.10–0.50 <sup>a</sup>	Calculated as ratio of noise at zero level to signal peak.
Water temperature <sup>†</sup>	0.40	From thermocouple specifications.
Optical absorption coefficient <sup>†</sup>	1.00	Random/repetitions.

<sup>a</sup> Depending on hydrophone

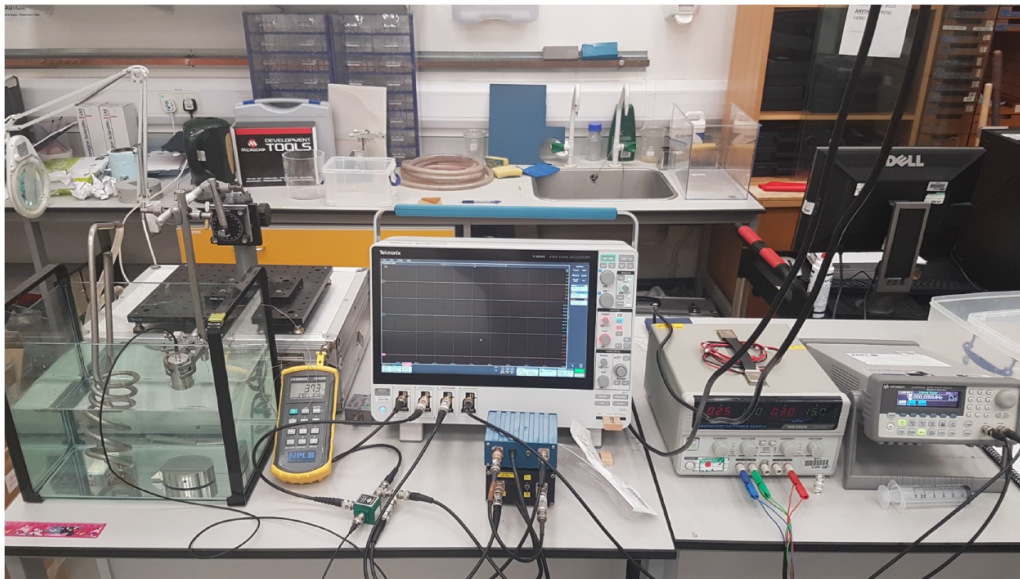
$J_p$  is known from the hydrophone specifications, where  $A = r^2\pi$  is the effective radiating surface, and the medium properties  $\rho$  (density) and  $c$  (speed of sound). A measurement of the input current  $I$  and received voltage  $U$  leads directly to the determination of acoustic pressure  $p$ , and thus  $S$  and  $M$ .

3.2. Measurement setup

In order to validate the LGUS method using self-reciprocity, the 5 mm piston hydrophone was used in the setup shown in figure 6. The hydrophone was held in a retort clamp connected to a manual rotation stage (RP01, Thorlabs Inc. Newton, NJ, USA) enabling precise tilt adjustments. The stage offers 360 ° of continuous rotation with a scale that is engraved in 1 ° increments along the outer circumference of the rotating platform. The hydrophone was immersed in a tank filled with degassed deionised water with electrical conductivity of 0.75 μS at 19 °C. The hydrophone was positioned perpendicularly above a reflecting target (98% reflectivity). The reflector satisfied the requirements set in K.5.5 of IEC 62127-2:2007 [2], including a diameter sufficient to encompass the entire ultrasonic beam and positioned at a distance from its surface of at least 1.5 times the near field distance, given by  $N_1 = a^2/\lambda$  where  $a$  is the effective radius of the ultrasonic transducer, and  $\lambda$  is the ultrasonic wavelength in water at its frequency of operation. The separation distance used in this case was thus 80 mm.



(a)



(b)

**Figure 6.** Self-reciprocity measurement setup with the schematic representation (a) and a photograph (b). The hydrophone is positioned perpendicularly above a reflecting target and the input as well as reflected signals are monitored by a current probe connected to an oscilloscope.

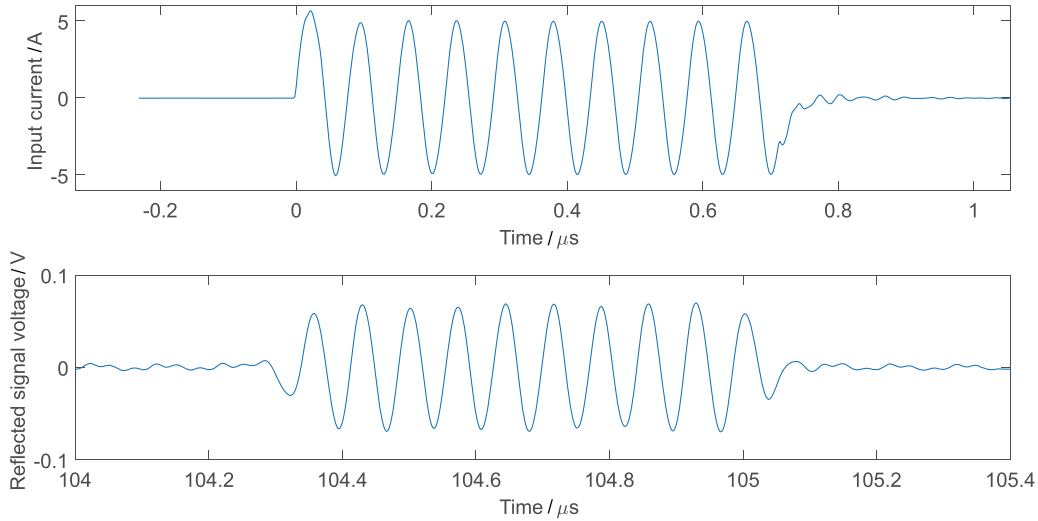


**Figure 7.** Input current to the hydrophone (top) and the reflected signal waveform (bottom) as monitored by the current probe connected to the oscilloscope.

The water (and thus hydrophone) temperature was changed in the range between 18 °C to 48 °C using the thermostat with an external temperature feedback as described in the previous section.

The hydrophone was excited by a 10 V peak-to-peak 10-cycle tone burst with 2 ms burst period at the hydrophone's centre frequency of 14 MHz provided by an arbitrary waveform generator (33 250A, Keysight Technologies, Santa Rosa, CA, USA). The input signal was monitored using an oscilloscope (MSO54, Tektronix Inc. Beaverton, OR, USA). The oscilloscope was set to 1000 averages, 6 kpts record length, 1.25 GS s<sup>-1</sup> sample rate and 480 ns div<sup>-1</sup> horizontal scale. An uncalibrated current probe (6027, Pearson Electronics, Palo Alto, CA, USA) was used to measure the input current to the transducer, as well as the reflected signals. The probe has nominally no impedance losses and has a conversion of 1 A = 1 V. The hydrophone was rotated and tilted in order to maximise the received signal. The input current ( $t = t_0$ ) to the hydrophone was kept constant with temperature and was 10 A peak-to-peak. The temperature-dependent reflected signals received after a delay ( $t = t_{\text{delay}}$ ) were low in amplitude so were amplified 5× and low-pass filtered (20 MHz) before the connection to the oscilloscope. The peak-to-peak amplitude of reflected signals at 22 °C was 0.14 V.

### 3.3. Data processing

The recorded time-domain signals were processed in MATLAB (R2020a, MathWorks, Massachusetts, USA) by first averaging the data and removing any DC offset. An example of the measured input current and reflected voltage signal at 22 °C is shown in figure 7. Only the stable middle part of the tone burst was used for analysis and the amplitude information for each time series extracted by taking the peak-to-peak amplitude of the signal. This method has sufficient accuracy for the signal-to-noise ratios obtained in the experiment.

The reciprocal coefficient for plane waves  $J_p$  depends on temperature due to the medium properties. This was calculated for water using the values as given in Jones and Harris (density [39]) and Marczak (speed of sound [22]). The acoustic pressure was then calculated using equation (3.1) as:

$$p = \sqrt{\frac{UI}{J_p}}. \quad (3.2)$$

The apparent value of the free-field voltage sensitivity  $M^*$  can then be calculated as  $M = \left| \frac{U}{p} \right|$ . Here, an ideal reflector is assumed as well as lossless transmission through the medium. In order to account for these, a correction factor  $k$  can be applied as defined in IEC 62127-2:2007 Annex K.11 [2], equation K.25. As the method used in this chapter was adapted to include a relative measurement across a wide range of temperatures, the factors contributing to the correction factor are reduced to include only the temperature dependent parameters, which are the amplitude reflection coefficient at the water/reflector surface  $R_{RT}$  and the acoustic attenuation  $\alpha(T)$ . The correction factor is then calculated as:

$$k(T) = \sqrt{\frac{1}{R_{RT}}} \exp(2d\alpha(T)) \quad (3.3)$$

where  $d$  is the distance between the hydrophone and reflector, while  $\alpha$  is the amplitude attenuation coefficient for ultrasound in pure, degassed water at 14 MHz. The corrected free-field sensitivity  $M_{\text{corr}}$  was then normalised to the value at 22 °C to yield the relative variation in sensitivity with temperature. Combined with the known hydrophone sensitivity at room temperature, this can be used to calculate the hydrophone's absolute sensitivity at a temperature  $T$ .

The expanded uncertainty was taken as the summation in quadrature of the uncertainty in hydrophone calibration and the overall systematic uncertainty of  $\pm 1.5$  dB in voltage

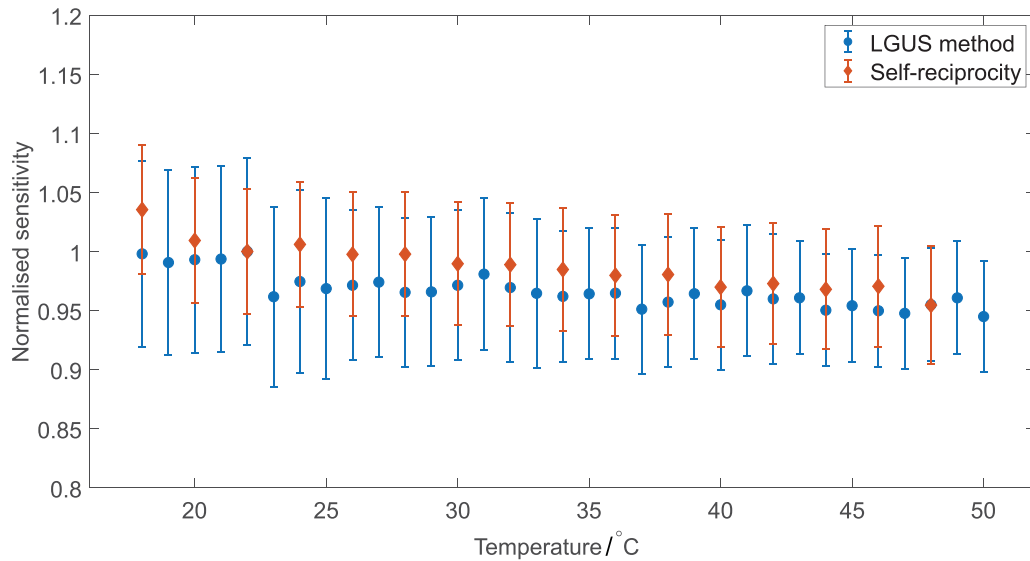


**Figure 8.** Relative change in hydrophone sensitivity with temperature as measured using the LGUS method (blue dots) and self-reciprocity (orange circles). The uncertainty bars represent the expanded uncertainty ( $p = 0.95$ ) and were calculated as described in table 1 and section 3.3 for the results acquired with the two methods, respectively.

sensitivity level as given in Clause K.8 of IEC 62127-2:2007 [2]. This was calculated as the ratio:

$$u_c(T) = \frac{-1.5dB(re1V/\mu Pa)}{20\log(M(T))} \quad (3.4)$$

where  $M(T)$  is the absolute temperature-dependent hydrophone sensitivity, thus yielding an expanded uncertainty of 5.2%.

## 4. Results and discussion

### 4.1. Validation using self-reciprocity

In order to validate the results obtained with the novel LGUS method, the variation in sensitivity of the 5 mm piston hydrophone was measured using both approaches. The measurements were performed at temperatures between 18 °C and 48 °C in steps of 2 °C using the self-reciprocity method, while for the LGUS method temperatures up to 50 °C were reached and data acquired every 1 °C. The relative values of free-field hydrophone sensitivity were obtained by normalising to temperature of 22 °C. Figure 8 shows the relative variation in sensitivity of the 5 mm piston hydrophone as measured using the self-reciprocity (orange diamonds) and LGUS (blue dots) approach. Both methods exhibit a small decreasing trend in the hydrophone sensitivity with temperature from 18 °C to 48 °C (50 °C in case of LGUS method), with trends of  $-0.19\%$  per °C ( $R^2: 0.89$ ) and  $-0.20\%$  per °C ( $R^2: 0.92$ ) (calculated using the slope of the weighted least-squares regression fit) for self-reciprocity and LGUS method,

respectively. The results show good agreement and are positioned within the uncertainty bars of both measurements, thus endorsing the validity of the results obtained with the LGUS method.

### 4.2. LGUS measurements

Once the approach to hydrophone calibration using a LGUS source was validated for the 5 mm piston hydrophone, two membrane hydrophones were also characterised. Figure 9 shows variations in sensitivity of the 1.0 mm bilaminar membrane hydrophone (a) and 0.2 mm differential membrane hydrophone (b) for temperatures from 17 °C to 37 °C in steps of 2 °C, as well as the piston hydrophone (c) for temperatures between 18 °C and 50 °C, normalised to 22 °C. The uncertainty bars represent the expanded uncertainty ( $p = 0.95$ ) evaluated as in section 2.8.

The sensitivity of the membrane hydrophones demonstrated a small variation with temperature, with a positive trend of approximately 0.08% per °C ( $R^2: 0.04$ ) for the bilaminar membrane hydrophone and 0.35% per °C ( $R^2: 0.048$ ) for the differential membrane hydrophone over the temperature range studied. The relatively low R-square values suggest that there may not be a significant change in sensitivity within this temperature range. Additionally, the temperature dependence of sensitivity for the 5 mm piston hydrophone was found to be approximately  $-0.20\%$  per °C (calculated using the fit slope,  $R^2: 0.92$ ) which is consistent with the observations reported in Kelley[8] regarding a reduction in normalised pulse-echo amplitude when the PVDF sensor is exposed to elevated temperatures.



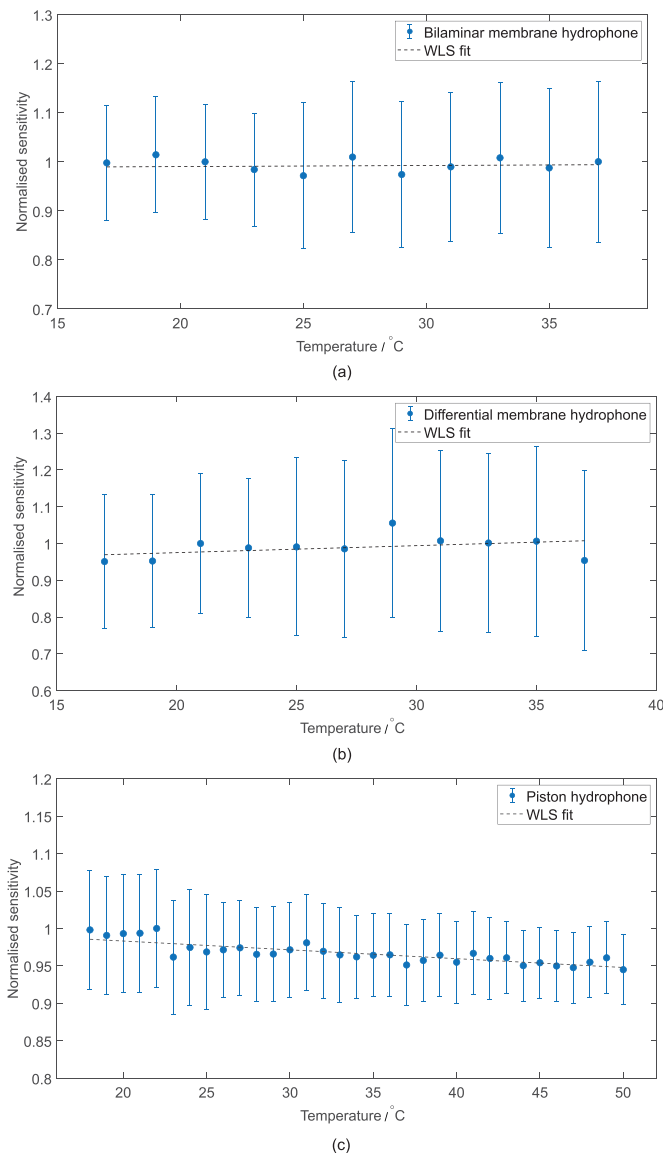


**Figure 9.** Relative change in sensitivity of the 1.0 mm bilaminar membrane hydrophone (a), 0.2 mm differential membrane hydrophone (b) and 5 mm piston hydrophone (c). All plots are normalised to 22 °C. Uncertainty bars represent the expanded uncertainty ( $p = 0.95$ ). The dotted lines represent the weighted least-squares (WLS) regression fit.

## 5. Summary and discussion

The knowledge of the variation in hydrophone sensitivity with temperature is important in order to reduce uncertainties in measurements made at temperatures different from those used for hydrophone calibration. In this work, a novel method for characterising the relative variation in hydrophone sensitivity with temperature was presented. A selection of hydrophones for medical applications was calibrated across the temperature range from 17 °C to 50 °C. The hydrophones exhibited a low temperature dependence within the measurement range consistent with the limited experimental data existing within

the literature. Previous measurements were limited to a smaller temperature range where the presence of random noise may have affected the observed slope. Whilst this does not provide a definitive conclusion on the variation in hydrophone sensitivity with temperature due to the limited number of devices tested in the study, it facilitates further studies on their behaviour by introducing a new measurement method. The different variation in sensitivity with temperature for different hydrophone types originates from the different temperature dependency of the dielectric constants for PVDF and water [4] but is also influenced by other factors such as electrical impedance and matching. The hydrophone geometry and mechanical features also make an important contribution, making modelling very difficult. As such, a direct measurement of the variation in hydrophone sensitivity is required. The LGUS method was validated using self-reciprocity as described in [15] and extended to include a relative measurement across a range of temperatures. This showed good agreement between the results obtained with both methods, thus endorsing the validity of results obtained with the new method.




Although temperature-dependent characterisation of hydrophone sensitivity can be achieved using the described self-reciprocity method, the LGUS method offers greater flexibility by allowing the characterisation of membrane hydrophones with small element sizes, which are typically unsuitable for the self-reciprocity approach due to limited energy transmission, as well as non-electrical transducers. The LGUS method uses the fundamental properties of water and provides the relative variation in hydrophone sensitivity with temperature, which can then be combined with the standard calibration at room temperature to determine absolute values. The experimental setup presented in this work serves to demonstrate the proposed method, highlight its underlying principles and showcase its capabilities within the limitations of the chosen configuration. Further modifications to the setup, such as changing the laser or incorporating optical lenses, have the potential to broaden the bandwidth of the LGUS source and enable data analysis in the frequency domain. This advancement would also enable exploration of the frequency-dependent nature of hydrophone sensitivity variation with temperature, opening avenues for future investigations.

## Acknowledgment

The authors would like to thank Dr Stephen Robinson from the National Physical Laboratory for his feedback on the manuscript.

This work was supported by the Engineering and Physical Sciences Research Council, UK.

## ORCID iDs

Marina Bakaric  <https://orcid.org/0000-0002-3609-311X>  
 Piero Miloro  <https://orcid.org/0000-0001-6809-2296>  
 Bradley E Treeby  <https://orcid.org/0000-0001-7782-011X>

## References

- [1] IEC 62127-1 2022 Ultrasonics - Hydrophones, Part 1: Measurement and Characterization of Medical Ultrasonic Fields International Electrotechnical Commission
- [2] IEC 62127-2 2017 Ultrasonics - Hydrophones, Part 2: Calibration for Ultrasonic Fields up to 40 MHz International Electrotechnical Commission
- [3] IEC 61689 2022 Ultrasonics. Physiotherapy Systems. Field Specifications and Methods of Measurement in the Frequency Range 0.5 International Electrotechnical Commission MHz to 5 MHz
- [4] Preston R, Robinson S, Zeqiri B, Esward T, Gélat P and Lee N 1999 *Metrologia* **36** 331
- [5] Robinson S, Preston R, Smith M and Millar C 2000 *IEEE Trans. Ultrason. Ferroelectr. Freq. Control* **47** 1336–44
- [6] Isaev A, Yi C, Matveev A and Zihong P 2015 *Metrologia* **52** 09001
- [7] Rajagopal S et al 2016 *Metrologia* **53** 09004
- [8] Kelley T 2018 *IET Sci. Meas. Technol.* **13** 370–4
- [9] Bakaric M, Fromme P, Hurrell A, Rajagopal S, Miloro P, Zeqiri B, Cox B T and Treeby B E 2021 *Ultrasonics* **114** 106378
- [10] Weber M and Wilkens V 2017 *Metrologia* **54** 432
- [11] Koch C and Molkenstruck W 1999 *IEEE Trans. Ultrason. Ferroelectr. Freq. Control* **46** 1303–14
- [12] Weber M and Wilkens V 2020 *IEEE Trans. Ultrason. Ferroelectr. Freq. Control* **68** 1919–29
- [13] Harris G R, Howard S, Hurrell A, Lewin P A, Schafer M E, Wear K A, Wilkens V and Zeqiri B 2022 *IEEE Trans. Ultrason. Ferroelectr. Freq. Control* **70** 85–100
- [14] Rajagopal S, de Melo Baesso R, Miloro P and Zeqiri B 2022 *IEEE Trans. Ultrason. Ferroelectr. Freq. Control* **70** 101–111
- [15] Beissner K 1980 *Acta Acust. U. Acust.* **46** 162–7
- [16] Wissmeyer G, Pleitez M A, Rosenthal A and Ntziachristos V 2018 *Light Sci. Appl.* **7** 1–16
- [17] Laufer J G, Elwell C E, Delpy D T and Beard P C 2004 Pulsed near-infrared photoacoustic spectroscopy of blood *Proc. SPIE* **5320** 57–68
- [18] Beard P 2011 *Interface Focus* **1** 602–31
- [19] Petrova E, Ermilov S, Su R, Nadvoretzkiy V, Conjusteau A and Oraevsky A 2013 *Opt. Express* **21** 25077–90
- [20] Chen S L 2017 *Appl. Sci.* **7** 25
- [21] Rajagopal S, Sainsbury T, Treeby B E and Cox B T 2018 *J. Acoust. Soc. Am.* **144** 584–97
- [22] Marczak W 1997 *J. Acoust. Soc. Am.* **102** 2776–9
- [23] Pinkerton J M 1949 *Proc. Phys. Soc. B* **62** 129
- [24] Wang L V and Wu H I 2012 *Biomedical Optics: Principles and Imaging* (Wiley)
- [25] Lemus R 2004 *J. Mol. Spectrosc.* **225** 73–92
- [26] Eisenberg D, Kauzmann W and Kauzmann W 2005 *The Structure and Properties of Water* (Oxford University Press on Demand)
- [27] Hale G M and Querry M R 1973 *Appl. Opt.* **12** 555–63
- [28] Palmer K F and Williams D 1974 *J. Opt. Soc. Am.* **64** 1107–10
- [29] Hale G M, Querry M R, Rusk A N and Williams D 1972 *J. Opt. Soc. Am.* **62** 1103–8
- [30] Irvine W M and Pollack J B 1968 *Icarus* **8** 324–60
- [31] Bakaric M 2022 Ultrasonography and phantom materials for validation of photoacoustic thermometry *Ph.D. Thesis* University College London
- [32] Smith R A and Bacon D R 1990 *J. Acoust. Soc. Am.* **87** 2231–43
- [33] Zeqiri B and Bond A D 1992 *J. Acoust. Soc. Am.* **92** 1809–21
- [34] Treeby B E, Wise E S, Kuklis F, Jaros J and Cox B 2020 *J. Acoust. Soc. Am.* **148** 2288–300
- [35] Treeby B E and Cox B T 2010 *J. Biomed. Opt.* **15** 021314
- [36] Shaw A and Hodnett M 2008 *Ultrasonics* **48** 234–52
- [37] Joint Committee for Guides in Metrology (JCGM) 2012 100 : 2012 Evaluation of measurement data - Guide to the expression of uncertainty in measurement (JCGM 2008 with minor corrections)
- [38] UKAS 2012 *The Expression of Uncertainty and Confidence in Measurement* 3rd edn Document No. M3003 (United Kingdom Accreditation Service (UKAS))
- [39] Jones F E and Harris G L 1992 *J. Res. Natl Inst. Stand. Technol.* **97** 335